We are IntechOpen,
the world's leading publisher of
Open Access books
Built by scientists, for scientists

4,800

Open access books available

122,000

International authors and editors

135M

Downloads

Our authors are among the

154

Countries delivered to

TOP 1%

most cited scientists

12.2%

Contributors from top 500 universities

CLARIVATE ANALYTICS
BOOK CITATION INDEX
INDEXED

WEB OF SCIENCE™

Selection of our books indexed in the Book Citation Index
in Web of Science™ Core Collection (BKCI)

Interested in publishing with us?
Contact book.department@intechopen.com

Numbers displayed above are based on latest data collected.
For more information visit www.intechopen.com

FEC Recovery Performance for Video Streaming Services Based on H.264/SVC

Kenji Kirihara, Hiroyuki Masuyama, Shoji Kasahara and Yutaka Takahashi
Kyoto University
Japan

1. Introduction

With the recent advancement of video coding techniques and wide spread use of broadband networks, video streaming services over the Internet have attracted considerable attention. The recent video streaming services cover multimedia messaging, video telephony, video conferencing, standard and high-definition TV broadcasting, and those services are provided over wired/wireless networks (Schwarz et al. 2007). The Internet, however, is a best-effort network, and hence the quality of service (QoS) for video streaming is not strictly guaranteed due to packet loss and/or delay. The varying connection quality of the Internet has accelerated the development of adaptive mechanisms of video coding technologies.

MPEG and H.26x are video coding standards which have been widely deployed. MPEG4's latest video codec is Part 10 or the advanced video codec (AVC), which is also identically standardized as ITU H.264 (Marpe et al. 2006). The fundamental coding mechanism of H.264/AVC consists of a Video Coding Layer (VCL) and a Network Abstraction Layer (NAL). The VCL generates a coded representation of a source content, and the resulting data is formatted with header information by the NAL. Pictures are partitioned into small coding units called macroblocks, which organized by the following three slices:

- I-slice: intra-picture predictive coding based on spatial prediction from neighboring regions.

- P-slice: intra-picture predictive coding and inter-picture predictive coding.

- B-slice: intra-picture predictive coding, inter-picture predictive coding, and inter-picture bi-predictive coding.

With these three types of slices, H.264/AVC succeeds in providing largely increased flexibility and adaptability in comparison with previous standards such as H.261, MPEG-1 Video, H.262, MPEG2 Video, H.263, and MPEG-4 Visual. The latest standardization effort addressing scalability is the extension of H.264/AVC called scalable video coding (SVC) (Schwarz et al. 2007; Wien et al. 2007). In 2007, the SVC scalability extension has been added to the H.264/AVC standard. In this paper, this extended version of H.264/AVC is referred to as H.264/SVC.

In (Van der Auwera et al. 2008a; Van der Auwera et al. 2008b), the fundamental traffic characteristics of H.264/AVC were extensively studied. It was reported that the bit rate variability for H.264/AVC is significantly higher than that for the MPEG-4 Part 2 encoder, particularly in the low to medium quality range. This large variability of H.264/AVC may

cause heavily bursty nature of packet traffic over the Internet. It is also expected that this bursty nature emerges even for the streaming services based on H.264/SVC.

Now consider H.264/SVC-based streaming services over the network consisting of optical backbone networks and low-speed access networks. Note that in this network, backbone edge routers are likely to be the bottleneck of the packet flows of H.264/SVC-based streaming services. It was reported in (Van der Auwera et al. 2008a) that the coefficient of variation (CoV) of the frame size increases as the video quality increases, indicating that the video traffic becomes more variable. Therefore, it is important to investigate the impact of the variability of the frame size on video quality.

In terms of the resilience to packet loss due to network congestion, there are two basic techniques for packet-loss recovery: Automatic Repeat reQuest (ARQ) and Forward Error Correction (FEC). ARQ is an acknowledgement-based error recovery technique, in which lost data packets are retransmitted by the sender host. However, this retransmission mechanism is activated by receiving duplicate acknowledgement (ACK) packets or timer time-out, causing a large end-to-end delay. This large delay is not suitable for real-time applications such as video streaming and web conference.

On the other hand, FEC is a well-known coding-based error recovery scheme (Carle & Biersack 1997; Perkins et al. 1998). FEC is a one-way recovery technique based on open-loop error control, and hence FEC is suitable for real-time applications. In FEC, redundant data is generated from original data, and both original and redundant data are transmitted to the receiver host. If the amount of lost data is less than or equal to a prespecified threshold, the lost data can be reconstructed on the receiver host. In this paper, we consider a packet-level FEC scheme (Shacham & Pckenney 1990). Because FEC needs no retransmission, it is suitable for real-time applications with stringent delay constraint such as video streaming. However, FEC does not work well against packet burst loss because the amount of redundant data has to be pre-determined with the estimate of the packet loss probability.

In this paper, focusing on the bottleneck router, we consider variable frame size's impact on frame loss. It is assumed that the number of packets in a frame is variable and that the interval of sending packets is constant on the transport layer. We model the bottleneck router as a single-server queueing system with two independent input processes: a general renewal input process for video streaming packets and a Poisson arrival process for background traffic multiplexed at the bottleneck router. Taking into account the variable nature of the number of packets in a frame, we derive the data-loss ratio of main traffic. In numerical examples, we investigate how the variability of the frame size affects the data-loss ratio. FEC recovery performance is also studied.

The rest of this paper is organized as follows. Section 2 shows related work, and in Section 3, we describe our analysis model, deriving the performance measure. Section 4 presents some numerical examples, and Section 5 concludes the paper.

2. Related work

H.264/AVC and its extension to the scalable video coding have been aggressively and extensively studied. The history of H.264/AVC and recent advancement toward SVC are well surveyed in (Schwarz et al. 2007).

It is well known that the traffic characteristics of encoded video have a significant impact on network transport. Its characteristics have been extensively studied in the literature. In particular, the authors in (Van der Auwera et al. 2008a; Van der Auwera et al. 2008b) compared H.264/AVC and MPEG4 Part 2 using two performance measures: the peak

signal-to-noise ratio (PSNR) and CoV of the frame size. They claimed that H.264/AVC codec can save the average bit rate more largely than MPEG4 Part 2 codec, and that the variability of H.264/AVC video traffic is higher than that MPEG4 Part 2 video traffic. They also examined how the frame-size smoothing is effective in mitigating the bit rate variability.

In general, video traffic exhibits a long-term correlation nature, which is hardly modeled with traditional Markovian arriving processes. In (Kempken et al. 2008), the authors considered discrete-time semi-Markov models of H.264/AVC video traffic. Focusing on the short term autocorrelation and the preservation of the mean value of the distribution of the size of group of pictures (GoP), the parameters of a discrete-time batch Markovian arrival process are optimized by simulated annealing approach.

In (Avramova et al. 2008), the tail probability of the queue length of a bottleneck router was studied with the effective bandwidth approach and trace-driven simulation experiments. In the effective bandwidth approach, the tail probability of the queue length can be well approximated when the number of input sources is large. The authors derived two estimates of the tail probability from two arrival processes: one is based on a fractional Brownian motion and the other a Markov-modulated fluid one. Those estimates were compared to trace-driven simulation.

In this paper, we focus on the multiplexing nature of the bottleneck router. In terms of this modeling point of view, the authors in (Muraoka et al. 2007) focused on the bottleneck edge router, evaluating the packet recovery performance of FEC for a single-server queueing system with finite buffer fed by two input processes: one is a general renewal input process, and the other is Poisson arrival process. Assuming that the packet size is exponentially distributed, the packet- and block-level loss probabilities were analyzed. In (Muraoka et al. 2009), the authors extended the model in (Muraoka et al. 2007) to a GI+M/SM/1/K queue in which the packet transfer time is governed by a two-state Markovian service process, investigating the recovery performance of FEC over wired-wireless networks. Note that in (Muraoka et al. 2007; Muraoka et al. 2009), the frame size is assumed to be constant. In this paper, we consider the case in which the frame size is variable.

3. Model and analysis

3.1 Variable frame size

We consider H.264/SVC-based streaming service. Each video frame contains original data packets and FEC redundant data packets, where the latter ones are generated from the former ones. The original data packets of a video frame is retrieved if the number of loss packets is less than or equal to that of the FEC redundant data packets. Otherwise the frame is lost. In what follows, we assume that the first packet of a video frame arrives to the bottleneck router at time $T_1 > 0$. The video frame is called "frame 1" hereafter. The subsequent video frames is called "frame 2", "frame 3", "frame 4" and so on. Let D_k ($k = 1, 2, \ldots$) denote the number of the original data packets in frame k. We assume that D_k's are independently and identically distributed (i.i.d.) with a probability mass function $d(n)$ ($n = 1, 2, \ldots$). We also assume that the number of FEC packets in frame k is equal to $\lceil \gamma D_k \rceil$, where $\gamma \geq 0$ denotes the redundancy. Thus the total number of packets in frame k is equal to $D_k + \lceil \gamma D_k \rceil$.

3.2 Model

We model the bottleneck router as a single-server queueing system with a buffer of capacity K, which is fed by two independent input processes. The one is a Poisson flow of packets in

background traffic, whose arrival rate is equal to λ. The other is a renewal packet flow of video frames from a streaming server, which is called main traffic. Let T_m's ($m = 2, 3, \ldots$) denote arrival epochs of main-traffic packets after the arrival of the first packet of frame 1 at time T_1, where $0 < T_1 < T_2 < T_3 < \cdots$. Note here that the first packet of frame k ($k = 1, 2, \ldots$) arrives at time T_{m_k}, where $m_k = \sum_{i=1}^{k-1}(D_i + \lceil \gamma D_i \rceil) + 1$. The interarrival times of packets in main traffic are i.i.d. with a general distribution $G(x)$ ($x \geq 0$), i.e., for each $m = 1, 2, \ldots$, $\Pr[\tau_m \leq x] = G(x)$ ($x \geq 0$), where $\tau_m = T_{m+1} - T_m$. The service times of packets in both main and background traffic are i.i.d. according to an exponential distribution with mean $1/\mu$. Consequently, we have a GI+M/M/1/K queueing system for the bottleneck router.

3.3 Stationary distribution of packets in the bottleneck router

This subsection considers the stationary queue length distribution immediately before an arrival from main traffic in the GI+M/M/1/K queueing system, which is described in the previous subsection. Recall that packets in main traffic arrive at times T_m's ($m = 1, 2, \ldots$). Let L_m^- ($m = 1, 2, \ldots$) denote the total number of packets in the system immediately before time T_m. Note that during the interval (T_m, T_{m+1}), the behavior of the GI+M/M/1/K queue is stochastically equivalent to that of the M/M/1/K queue with arrival rate λ and service rate μ. Thus $\{L_m^-; m = 1, 2, \ldots\}$ is a Markov chain whose transition probability matrix $\mathbf{\Pi}$ is given by

$$\mathbf{\Pi} = \mathbf{\Lambda} \int_0^\infty \exp(\mathbf{Q}x) \mathrm{d}G(x), \tag{1}$$

where $\mathbf{\Lambda}$ and $\mathbf{Q}$ denote $(K+1) \times (K+1)$ matrices that are given by

$$\mathbf{\Lambda} = \begin{pmatrix} 0 & 1 & 0 & \ldots & 0 & 0 \\ 0 & 0 & 1 & \ddots & 0 & 0 \\ \vdots & \vdots & \ddots & \ddots & \vdots & \vdots \\ 0 & 0 & 0 & \ddots & 1 & 0 \\ 0 & 0 & 0 & \ldots & 0 & 1 \\ 0 & 0 & 0 & \ldots & 0 & 1 \end{pmatrix}, \tag{2}$$

$$\mathbf{Q} = \begin{pmatrix} -\lambda & \lambda & 0 & \ldots & 0 & 0 \\ \mu & -(\lambda+\mu) & \lambda & \ddots & \vdots & \vdots \\ 0 & \mu & -(\lambda+\mu) & \ddots & 0 & 0 \\ 0 & 0 & \mu & \ddots & \lambda & 0 \\ \vdots & \vdots & \ddots & \ddots & -(\lambda+\mu) & \lambda \\ 0 & 0 & 0 & \ddots & \mu & -\mu \end{pmatrix}.$$

Note here that $\mathbf{\Pi}$ is aperiodic. Let $\boldsymbol{\pi}$ denote a $1 \times (K+1)$ probability vector whose jth ($j = 0, 1, \ldots, K$) element π_j represents $\lim_{m \to \infty} \Pr[L_m^- = j]$. We then have

$$\boldsymbol{\pi}\mathbf{\Pi} = \boldsymbol{\pi}, \qquad \boldsymbol{\pi}e = 1,$$

where e denotes a column vector of ones with appropriate dimension.

3.4 Derivation of data-loss ratio

This subsection derives the long-term ratio P_{data} of the number of unretrieved data packets to that of all the original data packets. Let $N(t)$ $(t \geq 0)$ denote the total number of video frames arriving to the system in the time interval $(0, t]$. Without loss of generality, we assume $N(0) = 0$. Let X_k $(k = 1, 2, \dots)$ denote the number of lost packets among frame k. The formal definition of P_{data} is as follows:

$$P_{data} = 1 - \lim_{t \to \infty} \frac{\sum_{k=1}^{N(t)} D_k \cdot 1(X_k \leq \lceil \gamma D_k \rceil)}{\sum_{k=1}^{N(t)} D_k},$$

where $1(\chi)$ denotes the indicator function of event χ. Let Q_k^- $(k = 1, 2, \dots)$ denote the number of packets in the system immediate before the arrival of the first packet of frame k. By definition (see subsection 3.2), $Q_k^- = L_{m_k}^-$ for $k = 1, 2, \dots$. Therefore $\lim_{k \to \infty} \Pr[Q_k^- = i] = \lim_{m \to \infty} \Pr[L_m^- = i] = \pi_i$ for all $i = 0, 1, \dots, K$. Note here that $\{(D_k, Q_k^-); k = 1, 2, \dots\}$ is a Markov renewal process because $\{D_k; k = 1, 2, \dots\}$ is a sequence of i.i.d. random variables and independent of a Markov chain $\{Q_k^-; k = 1, 2, \dots\}$. Note also that each $D_k \cdot 1(X_k \leq \lceil \gamma D_k \rceil)$ can be regarded as *reward* depending on D_k and Q_k^-. It then follows from the Markov renewal reward theorem (Wolf 1989) that

$$P_{data} = 1 - \frac{E_\pi[D_1 \cdot 1(X_1 \leq \lceil \gamma D_1 \rceil)]}{E[D_1]}, \tag{3}$$

where $E_\pi[\cdot] = \sum_{i=0}^{K} \pi_i E[\cdot \mid Q_1^- = i]$. From (3) and $Q_1^- = L_1^-$, we have

$$P_{data} = 1 - \frac{\sum_{i=0}^{K} \pi_i \sum_{n=1}^{\infty} nd(n) \Pr[X_1 \leq \lceil \gamma n \rceil \mid D_1 = n, L_1^- = i]}{\sum_{n=1}^{\infty} nd(n)}$$

$$= 1 - \frac{\sum_{n=1}^{\infty} nd(n) \cdot \sum_{i=0}^{K} \pi_i q(\lceil \gamma n \rceil; n, i)}{\sum_{n=1}^{\infty} nd(n)}, \tag{4}$$

where $q(\nu; n, i)$ $(\nu = 0, 1, \dots, n, n = 1, 2, \dots, i = 0, 1, \dots, K)$ denotes

$$q(\nu; n, i) = \Pr[X_1 \leq \nu \mid D_1 = n, L_1^- = i]. \tag{5}$$

We can readily compute $\sum_{i=0}^{K} \pi_i q(\lceil \gamma n \rceil; n, i)$ by the recursion given in subsection 3.2 of (Muraoka et al. 2007), because $\sum_{i=0}^{K} \pi_i q(\lceil \gamma n \rceil; n, i)$ is equivalent to $\sum_{k=0}^{\lceil \gamma n \rceil} p_{n + \lceil \gamma n \rceil}(k)e$ therein.

4. Numerical examples

In this section, we evaluate the impact of the variable frame size using the data-loss ratio derived in the previous section. The transmission rate of video streaming service is set to 20 Mbps, and the output transmission speed of the bottleneck router is 100 Mbps. We consider two system capacity cases: $K = 10$ and 100. It is assumed that the video-frame rate is 30 [frame/s], and that the packet size is constant and equal to 500 bytes. Then, the service rate of a packet at the bottleneck router is $\mu = 2.5 \times 10^4$ [packet/s].

We assume that the packet interarrival time of main traffic is constant. Let $D_{\min}$ ($D_{\max}$) denote the minimum (maximum) value of the frame size. In terms of $d(n)$, we consider the following uniform distribution.

$$d(n) = \begin{cases} 1/(D_{\max} - D_{\min} + 1), & D_{\min} \leq n \leq D_{\max}, \\ 0, & 0 \leq n < D_{\min}, n > D_{\max}. \end{cases}$$

Type	Main traffic	$\bar{M}$	D_{min}	D_{max}	CoV
I	20 Mbps	167	151	183	0.0570
II	20 Mbps	167	39	295	0.442

Table 1. Basic parameters for uniform distribution.

Name	Original filename	Date/Cpat.on	Duration
Leipzig-II	20030221-121359-0.g2	February 21 12:13:59 2003	164min
Leipzig-II	20030222-150000-0.g2	February 22 15:00:00 2003	360min

Table 2. General information about the trace used for simulation experiments.
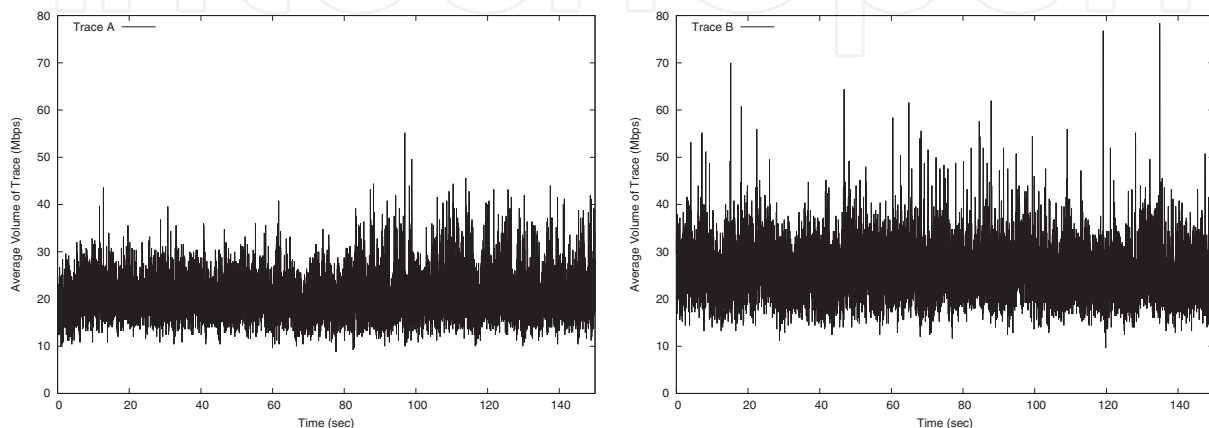
Fig. 1. The average bit rate of trace data.

The basic parameter set is shown in Table 1. In the following, we denote CoV as the coefficient of variation of the frame size. Let $\bar{M}(\gamma)$ denote the average of the number of packets in a frame, which is given by

$$\bar{M}(\gamma) = \sum_{n=1}^{\infty} (n + \lceil \gamma n \rceil) d(n).$$

When the video transmission rate is 20 Mbps, the mean number of original data packets in a frame is $\bar{M}(0) = 167$.

We validate the analytical model by simulation experiments driven by traces of the NLANR repository (PMA). The trace data was used for the inter-arrival times of background traffic, and the other settings are the same as the analysis. Table 2 shows the details of the trace data used for simulation experiments in this paper. The subset of each trace data was used for the simulation experiment. In the following, we call the trace data from 20030222-150000-0.g2 (resp. 20030221-121359-0.g2) is called Trace A (resp. Trace B). Each trace was used for the inter-arrival times of packets in background traffic.

Figure 1 shows the average bit rate of the trace data. Note that Trace B represents the trace data whose volume varies greatly. Figure 2 illustrates the histogram of the trace data. The left-hand (resp. right-hand) figure in Fig. 2 shows the histogram of Trace A (resp. Trace B). When the packet size is 500 bytes, the volume of Trace A (resp. Trace B) is equal to 20.3 Mbps (resp. 25.5 Mbps) and the corresponding arrival rate λ is 5.09×10^3 (resp. 6.37×10^3) [packet/s]. The average of the packet inter-arrival times for Trace A (resp. Trace B) is 1.97×10^{-1} (resp. 1.56×10^{-1}). The variance of the packet inter-arrival times for Trace A (resp. Trace B) is 4.56×10^{-2} (resp. 3.11×10^{-2}). The resulting CoV of the packet inter-arrival times for Trace A (resp. Trace B) is 1.08 (resp. 1.13).
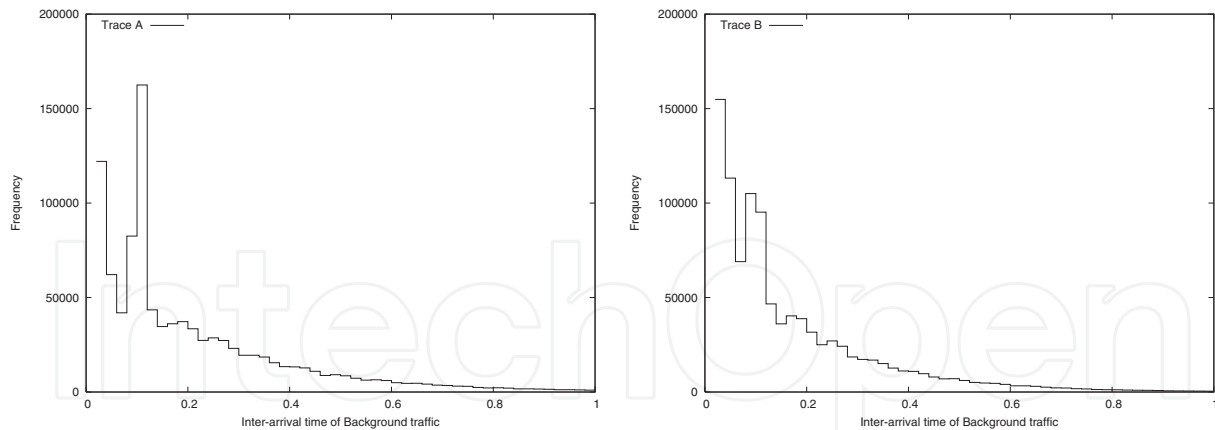
Fig. 2. Histogram of trace data.

4.1 Impact of system capacity

In this subsection, we investigate how the system capacity affects the data-loss ratio. In the following figures, analytical results are shown with lines, compared with simulation results represented by dots with 95% confidence intervals.
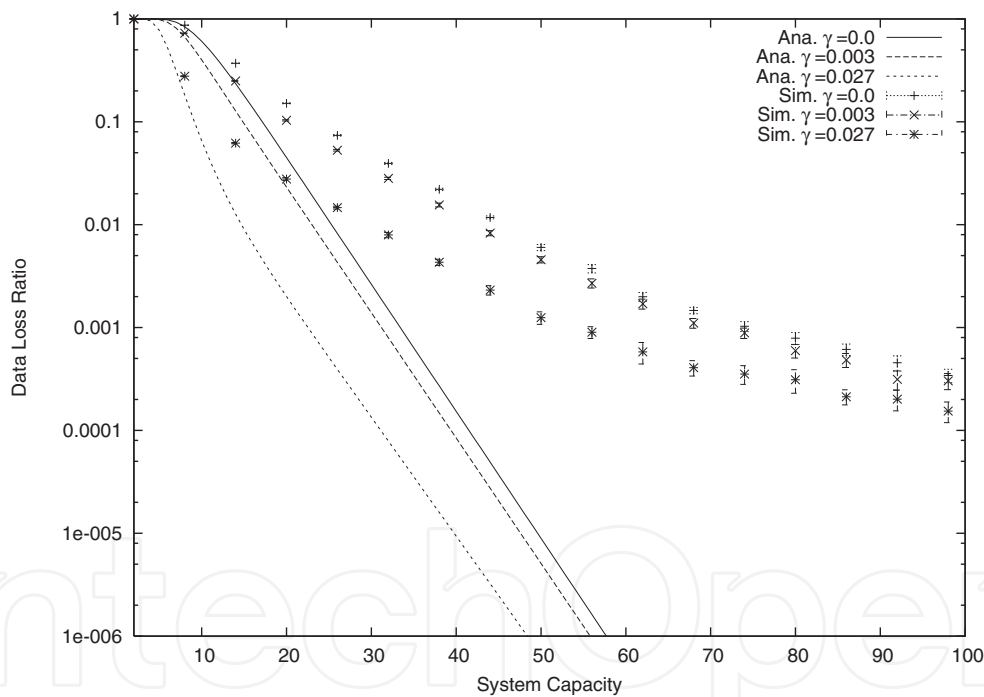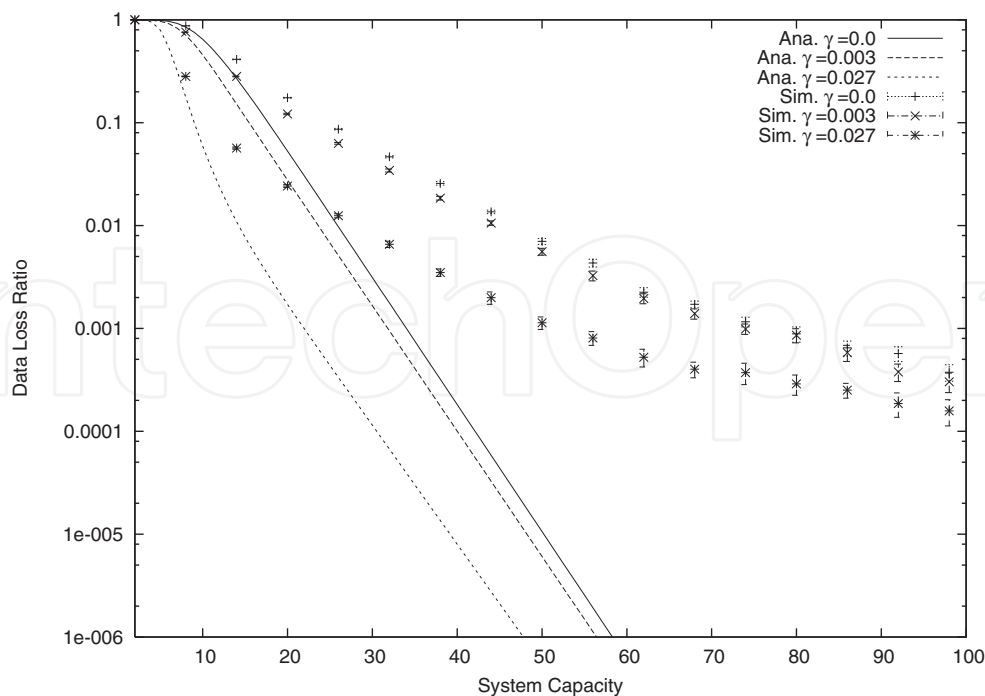

Fig. 3. System capacity vs. data-loss ratio. (The transmission rate 50 Mbps, main traffic 20 Mbps, Trace A, Type I)

Figure 3 (4) shows the data-loss ratio against the system capacity K when the frame size distribution is Type I (II). We calculated the data-loss ratio for $\gamma = 0$, 0.003 and 0.027. Note that the corresponding value of $\bar{M}(\gamma)$ is $\bar{M}(0) = 167$, $\bar{M}(0.003) = 168$ and $\bar{M}(0.027) = 172$. Here, the transmission rate of the bottleneck router is 50 Mbps, and the packet arrival rate of background traffic is 5.09×10^3 [packet/s], the mean packet arrival rate of Trace A.

In Figure 3, for each γ, simulation results are greater than analytical results. In addition, the discrepancy between analysis and simulation is large even for a small K. This is because the packet interarrival times of the trace data used for background traffic in simulation are more

Fig. 4. System capacity vs. data-loss ratio. (The transmission rate 50 Mbps, main traffic 20 Mbps, Trace A, Type II)

correlated than the Poisson process assumed for the analytical model. We also observe that the data-loss ratio decreases with the increase in K, as expected. The data-loss ratio is decreased by FEC, however, increasing the system capacity is more effective than FEC.

Comparing Figures 3 and 4, we observe that when CoV is large, the data-loss ratio for a large FEC redundancy is slightly smaller than that for a small FEC redundancy. This implies that FEC is effective for the video transmission in which the video frame size has a large variability. Figure 5 (6) shows the data-loss ratio against the system capacity K when the frame size distribution is Type I (II). Most of the parameters are the same as Figure 3 (4), except that the packet arrival rate of background traffic is 6.37×10^3 [packet/s], the mean packet arrival rate of Trace B. Note that the CoV of the packet inter-arrival times for Trace B is larger than that for Trace A. From Figures 5 and 6, we observe the same tendencies as Figures 3 and 4. From these results, we can claim that the analysis is useful in a qualitative sense to investigate the effect of the variability of the frame size on the data-loss ratio.

4.2 Impact of variable frame size

In this subsection, we investigate how the variable frame size affects the data-loss ratio. It is supposed that the transmission rate of the bottleneck router is 50 Mbps (100 Mbps). Thus the packet service rate of the bottleneck router is $\mu = 1,25 \times 10^4$ (2.5×10^4) [packet/s].

Figures 7 and 8 illustrate the data-loss ratio against the CoV of the frame size in case of the K=10 and 40. In each K, we calculated the data loss ratio for $\gamma = 0$, 0.003 and 0.027. Note that the corresponding value of $\bar{M}(\gamma)$ is $\bar{M}(0) = 167$, $\bar{M}(0.003) = 168$ and $\bar{M}(0.027) = 172$. In order to change the value of CoV, we decrement (increment) $D_{\min}$ ($D_{\max}$) by one, keeping the mean frame size constant.

In Figure 7, the data-loss ratio grows monotonically with the increase in CoV in cases of γ=0 and 0.003. This is simply due to a small FEC redundancy. On the other hand, the data-loss ratio gradually decreases when the redundancy γ is 0.027. In Figure 8, we observe similar
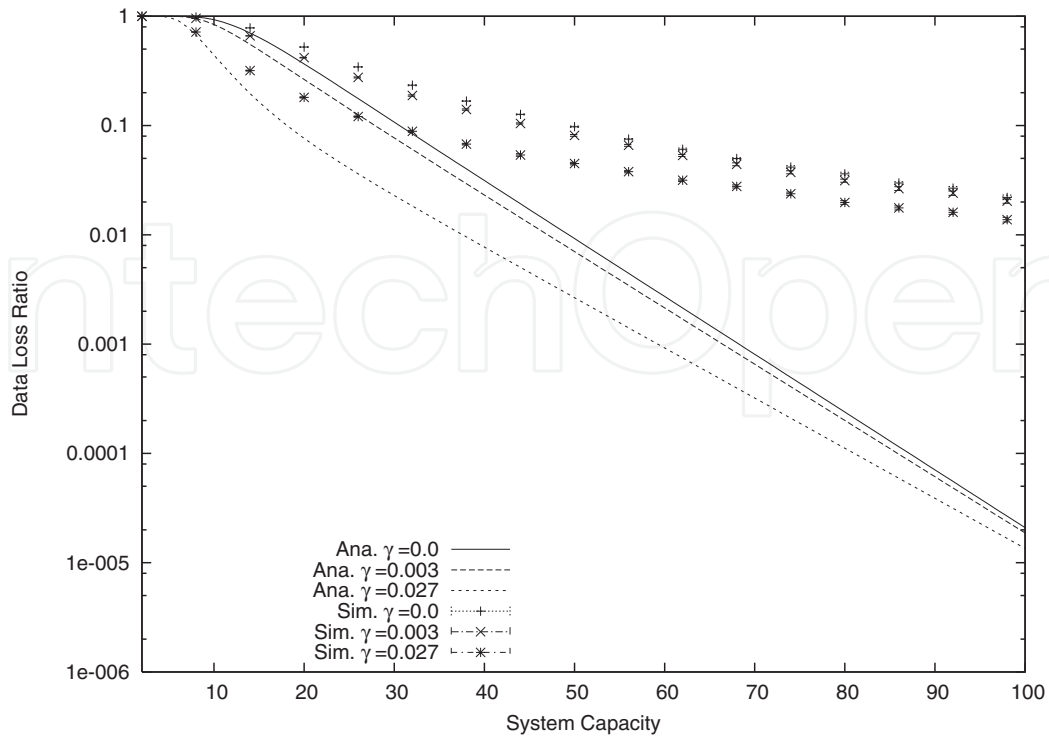
Fig. 5. System capacity vs. data-loss ratio. (The transmission rate 50 Mbps, main traffic 20 Mbps, Trace B, Type I)
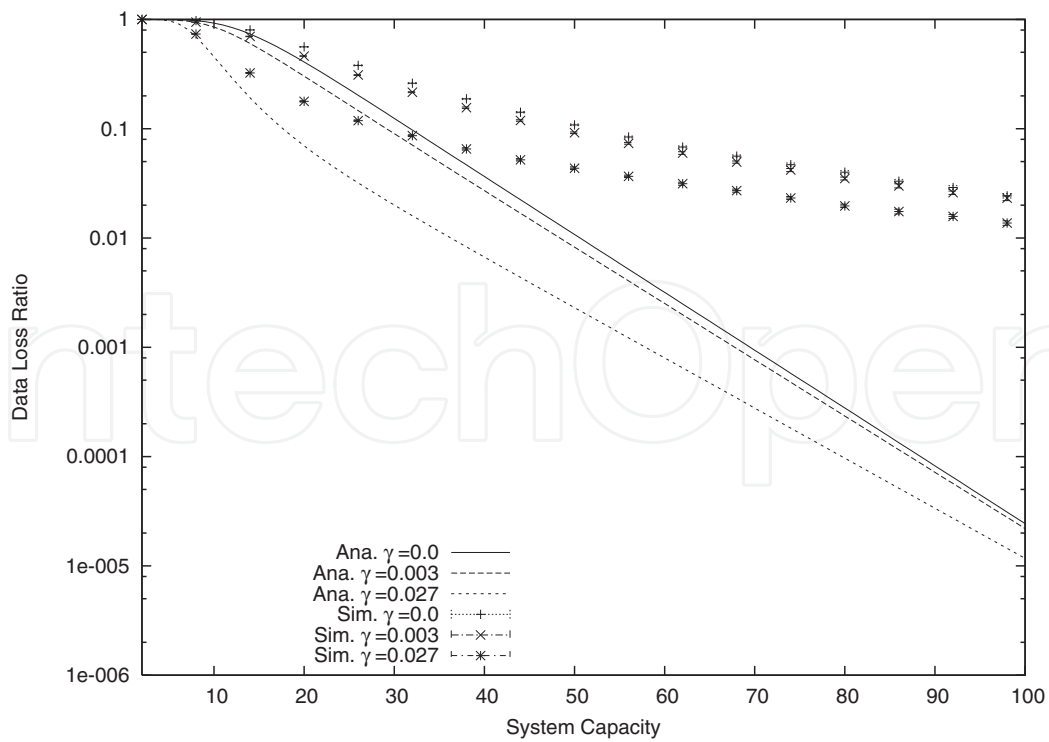

Fig. 6. System capacity vs. data-loss ratio. (The transmission rate 50 Mbps, main traffic 20 Mbps, Trace B, Type II)

characteristics as Figure 7. Note that the data-loss ratio in Figure 8 is smaller than that in Figure 7 and the impact of the variable frame size is small.

Figures 9 and 10 illustrate the data-loss ratio against the frame size in cases of $K =10$ and 20. Here, the transmission rate of the bottleneck router is 100 Mbps. In Figure 9, when $\gamma=0$ and 0.003, the data-loss ratio gradually grows with the increase in CoV, so the tendency is similar to the case where the transmission rate of the bottleneck router is 50 Mbps. In case of $\gamma=0.027$, on the other hand, the data-loss ratio increases step by step when the CoV increases. The data-loss ratio of a large CoV is about 400 times larger than that of a small CoV. In other words, when the FEC redundancy increases, the data-loss ratio becomes small but is significantly affected by CoV. In Figure 10, we observe the same characteristics as Figure 9. Note that the data-loss ratio is more improved for the system with a large capacity.

4.3 Impact of background traffic

In this subsection, we investigate how the data-loss ratio is affected by the volume of background traffic. Figure 11 represents the data-loss ratio against the volume of background traffic in cases of $K = 10$ and 100. In terms of $d(n)$, we consider Types I and II. The FEC redundancy γ is set to 0 and 0.027. It is observed that the data-loss ratio grows with the increase in the volume of background traffic, as expected. When K is small, FEC is effective in decreasing the data-loss ratio. However, the data-loss ratio for a large FEC redundancy is significantly affected by CoV. When K is large, on the other hand, the data-loss ratio is significantly improved. This implies that increasing the buffer size is more effective than FEC for a bottleneck router in congestion.
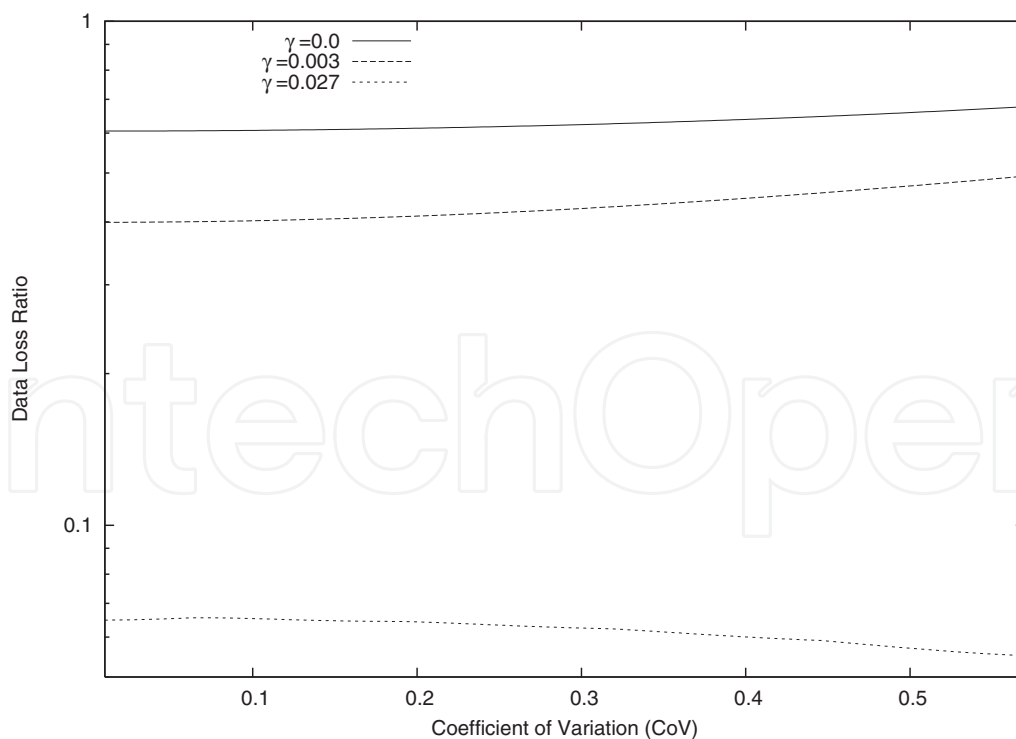

Fig. 7. CoV vs. the data-loss ratio. (The transmission rate 50 Mbps, background traffic 20.3 Mbps, $K = 10$)
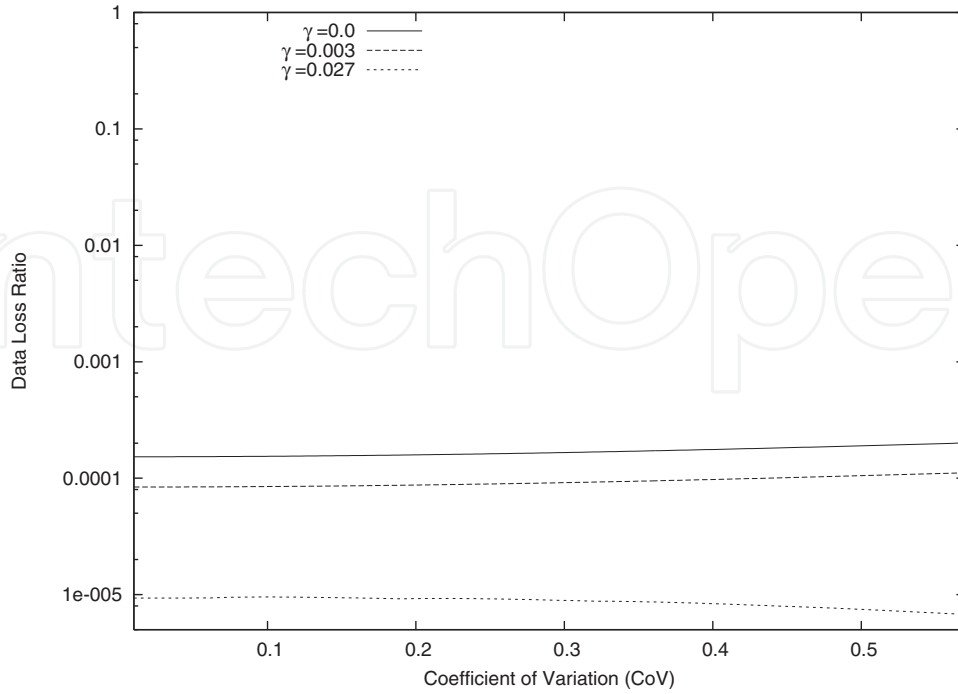
Fig. 8. CoV vs. the data-loss ratio. (The transmission rate 50 Mbps, background traffic 20.3 Mbps, $K = 40$)
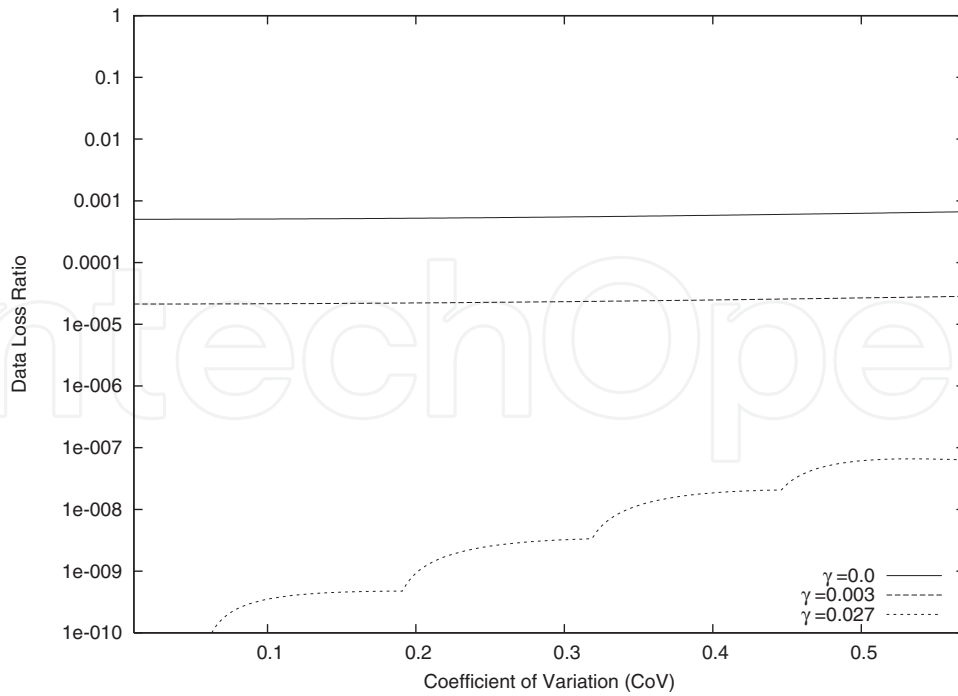

Fig. 9. CoV vs. the data-loss ratio. (The transmission rate 100 Mbps, background traffic 20.3 Mbps, $K = 10$)
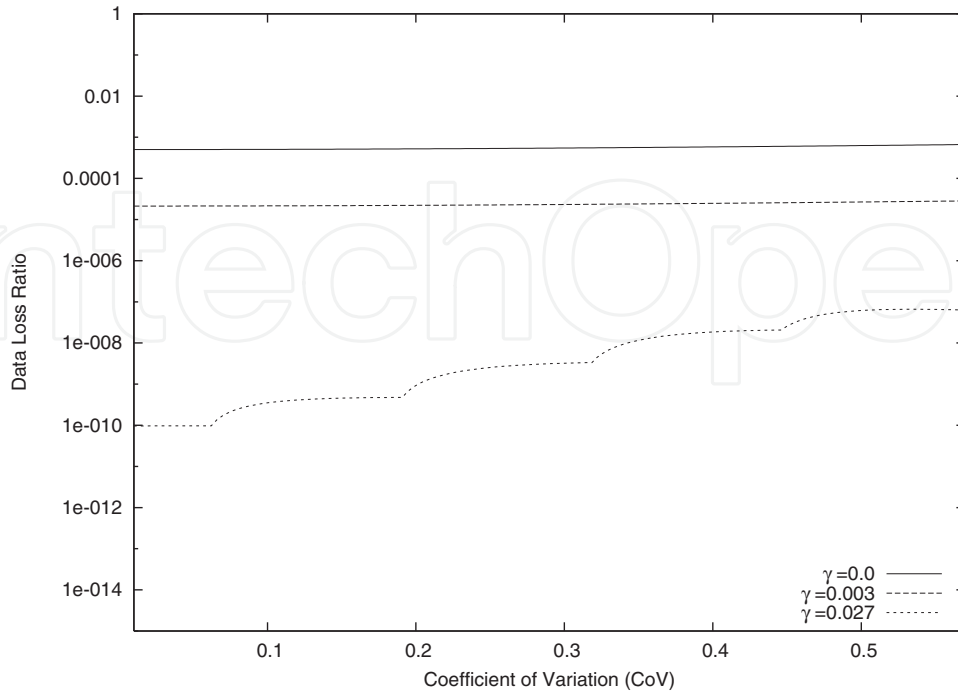
Fig. 10. CoV vs. the data-loss ratio. (The transmission rate 100 Mbps, background traffic 20.3 Mbps, $K = 20$)
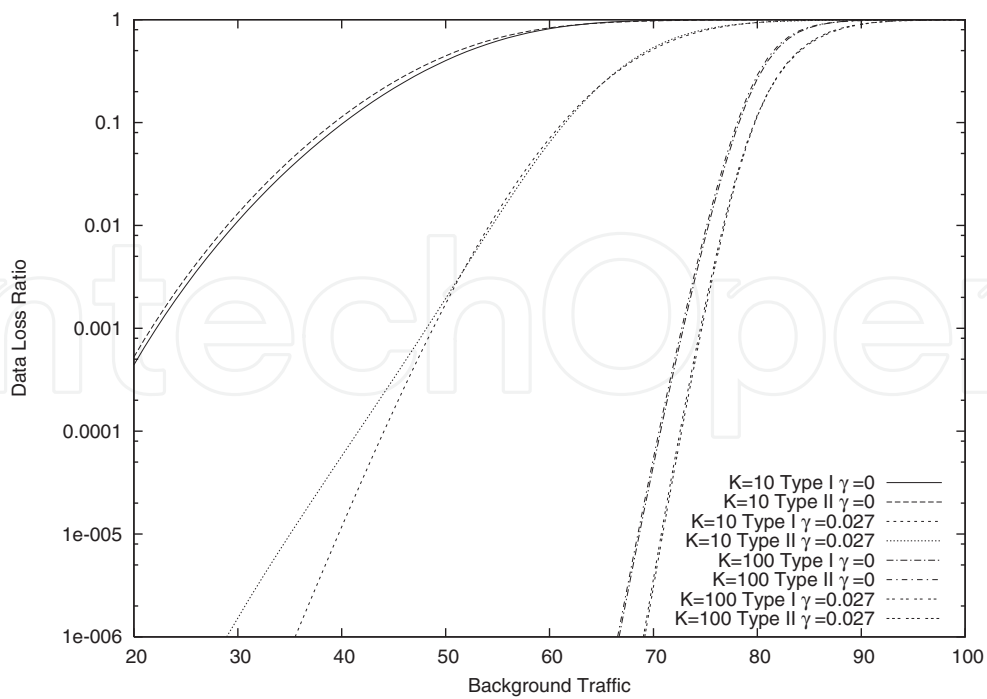

Fig. 11. Background traffic vs. the data-loss ratio.

5. Conclusions

In this paper, focusing on the bottleneck router, we considered the impact of the frame-size variability on frame loss. We modeled the bottleneck router as a single-server queueing system with two independent input processes: a general renewal input process and a Poisson arrival process, deriving the data-loss ratio of main traffic. The analysis was validated in a qualitative sense by trace-driven simulation. Numerical examples showed the data-loss ratio is not significantly affected by the variability of the frame size. It was also claimed that increasing the buffer size is more effective than FEC for a bottleneck router in congestion.

6. References

[Avramova et al. 2008] Avramova, Z., De Vleeschauwer, D., Laevens, K., Wittevrongel, S. & Bruneel, H. (2008). Modelling H.264/AVC VBR video traffic: comparison of a Markov and a self-similar source model, *Telecommunication Systems*, 39 (2): 91-102.

[Carle & Biersack 1997] Carle, G. & Biersack, E. W. (1997). Survey on error recovery techniques for IP-based audio-visual multicast applications, *IEEE Network Magazine*, 11 (6): 24–36.

[Kempken et al. 2008] Kempken, S., Hasslinger, G. & Luther, W. (2008). Parameter estimation and optimization techniques for discrete-time semi-Markov models of H.264/AVC video traffic, *Telecommunication Systems* 39 (2): 77–90.

[Marpe et al. 2006] Marpe, D., Wiegand, T. & Sullivan, G. (2006). The H.264/MPEG4 advanced video coding standard and its applications, *IEEE Communications Magazine*, 44 (8): 134–143.

[Muraoka et al. 2007] Muraoka, S., Masuyama, H., Kasahara, S. & Takahashi, Y. (2007). Performance analysis of FEC recovery using finite-buffer queueing system with general renewal and Poisson inputs, *Proceedings of Managing Traffic Performance in Converged Networks*, LNCS4516, Springer, 707–718.

[Muraoka et al. 2009] Muraoka, S., Masuyama, H., Kasahara, S. & Takahashi, Y. (2009). FEC recovery performance for video streaming services over wired-wireless networks, *Performance Evaluation*, 66 (6): 327–342.

[Perkins et al. 1998] Perkins, C., Hodson, O. and Hardman, V. (1998). A survey of packet loss recovery techniques for streaming audio, *IEEE Network Magazine*, 12 (5): 40–48.

[Schwarz et al. 2007] Schwarz, H., Marpe, D. & Wiegand, T. (2007). Overview of the scalable video coding extension of the H.264/AVC standard, *IEEE Transactions on Circuits and Systems for Video Technology* 17 (9): 1103–1120.

[Shacham & Pckenney 1990] Shacham, N. & Pckenney, P. (1990). Packet recovery in high-speed networks using coding and buffer management," *Proceedings of IEEE INFOCOM* 1: 124–131.

[Van der Auwera et al. 2008a] Van der Auwera, G., David, P. T. & Reisslein, M. (2008). Traffic and quality characterization of single-layer video streams encoded with the H.264/MPEG-4 advanced video coding standard and scalable video coding extension, *IEEE Transactions on Broadcasting* 54 (3): 698–718.

[Van der Auwera et al. 2008b] Van der Auwera, G., David, P. T. & Reisslein, M. (2008). Traffic characteristics of H.264/AVC variable bit rate video, *IEEE Communications Magazine* 46 (11): 164–174.

[Wien et al. 2007] Wien, M., Schwarz, H. & Oelbaum, T. (2007). Performance analysis of SVC, *IEEE Transactions on Circuits and Systems for Video Technology* 17 (9): 1194–1203.

[Wolf 1989] Wolff, R. W. (1989). *Stochastic modeling and the theory of queues*, Prentice-Hall.
[PMA] Passive   Measurement   and   Analysis   (PMA).   URL: http://pma.nlanr.net
        /Special/leip2.html

Recent Advances on Video Coding

Edited by Dr. Javier Del Ser Lorente

This book is intended to attract the attention of practitioners and researchers from industry and academia interested in challenging paradigms of multimedia video coding, with an emphasis on recent technical developments, cross-disciplinary tools and implementations. Given its instructional purpose, the book also overviews recently published video coding standards such as H.264/AVC and SVC from a simulational standpoint. Novel rate control schemes and cross-disciplinary tools for the optimization of diverse aspects related to video coding are also addressed in detail, along with implementation architectures specially tailored for video processing and encoding. The book concludes by exposing new advances in semantic video coding. In summary: this book serves as a technically sounding start point for early-stage researchers and developers willing to join leading-edge research on video coding, processing and multimedia transmission.

How to reference

In order to correctly reference this scholarly work, feel free to copy and paste the following:

Kenji Kirihara, Hiroyuki Masuyama, Shoji Kasahara and Yutaka Takahashi (2011). FEC Recovery Performance for Video Streaming Services Based on H.264/SVC, Recent Advances on Video Coding, Dr. Javier Del Ser Lorente (Ed.), ISBN: 978-953-307-181-7, InTech, Available from: http://www.intechopen.com/books/recent-advances-on-video-coding/fec-recovery-performance-for-video-streaming-services-based-on-h-264-svc

INTECH
open science | open minds